FERMILAB-CONF-08-344-E

Hadron Collider Physics Symposium (HCP2008), Galena, Illinois, USA

W boson mass measurement at the Tevatron

I. Bizjak (for the CDF Collaboration)
University College London, Gower Street, LONDON, WC1E 6BT, UK *

The mass of the W boson is one of the least precisely measured parameters of the electroweak interaction. Confronted with other measurements of standard model parameters it can test the internal consistency of the Standard Model and can constrain the possible mass of the standard model Higgs boson. The CDF collaboration has published the current single most precise measurement of the W boson mass using 200 pb^{-1} of CDF Run II $p\bar{p}$ data, and an improved measurement with 2.4 fb^{-1} of CDF Run II data is underway. Both measurements are described in detail in these proceedings.

1. INTRODUCTION

The standard model of particle physics (SM) has been very successful in describing electroweak interactions. The mass of the W boson is one of the parameters of the electroweak theory, which at tree level is fully determined by the relations to the other electroweak parameters. The loop corrections to the W boson mass calculation are dominated by the loop containing the b and t quarks and could receive a contribution from a loop with the yet-unconfirmed Higgs boson, while further corrections can come from loops with possible supersymmetric particles. Precision measurements of the W boson mass allow us to constrain the size of the possible loop corrections, giving us valuable information on the range of possible Higgs masses. The proceedings present one of the most precise single measurements of the W boson mass.

2. THE W BOSON MASS MEASUREMENT AT CDF

The Tevatron experiments CDF and DØ have long been involved in the measurement of the W boson mass, first pushing the precision below 100 MeV/c^2, and later published the combined average of the Run I W boson mass with an uncertainty of 59 MeV/c^2 [1]. In 2001 the upgraded CDF and DØ detectors began taking data and the size of the Run I dataset has long been surpassed. The CDF detector uses its tracking and calorimetry capabilities to measure the W boson mass both in $W \to e\nu$ and $W \to \mu\nu$ decays.

2.1. Measurement Strategy

The W bosons in $p\bar{p}$ collisions are mainly produced in quark anti-quark annihilation. In the environment of hadronic machines, only $W \to e\nu$ and $W \to \mu\nu$ decays can be reconstructed with the purity needed for the W boson mass measurement. The neutrino is not detected in the CDF detector and its momentum cannot be fully kinematically constrained, since the momentum of the incoming partons producing the W boson is not known, and the momentum along the beam-line cannot be accurately measured. The momentum conservation of the measured quantities can instead be applied in the transverse plane, since the partons have negligible transverse momenta. The transverse momentum of the neutrino (p_T^ν) is thus inferred from $\not\!\!E_T$, the missing transverse momentum required to achieve

*On leave from J. Stefan Institute, Jamova 39, Ljubljana, Slovenia.

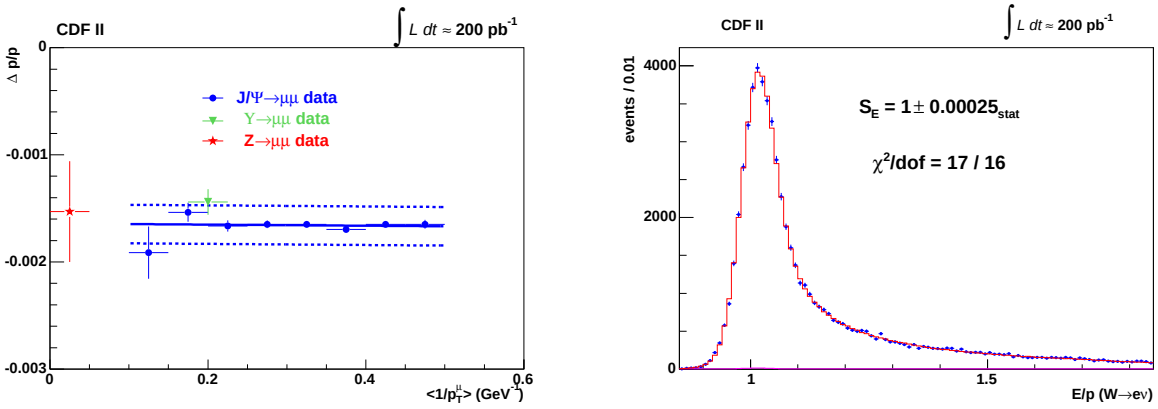

(a) (b)

Figure 1: (a) The fractional momentum correction $\Delta p/p$ as a function of the mean inverse momentum of the muons from $J/\psi \to \mu^+\mu^-$, $\Upsilon(1S) \to \mu^+\mu^-$ and $Z \to \mu^+\mu^-$ decays. The full line is the best linear fit to the points, and the dotted lines mark the total (statistical and systematic) uncertainty of the fit. (b) The E/pc distribution used for the calibration of the energy measurement.

the momentum balance in the transverse plane. The so-called transverse mass is constructed out of the kinematic quantities in the transverse plane:

$$m_T = \sqrt{2p_T^l \cdot p_T^\nu \cdot [1 - \cos(\phi_\ell - \phi_\nu)]} \quad . \tag{1}$$

The dependence of m_T on m_W is determined using Monte Carlo (MC) templates, which are created for different input m_W. The template best corresponding to the data distributions is extracted by a binned maximum-likelihood fit. The W boson mass is also obtained from the templates constructed for lepton transverse momentum p_T^l and the transverse momentum of the neutrino, $\not\!\!E_T$. The final m_W value is a weighted average of the three determinations. While the three variables are highly correlated, they have different sensitivities to boosts and systematic effects, hence their combination improves the m_W determination.

For the desired accuracy of the m_W measurement the m_T, p_T^l, and $\not\!\!E_T$ templates need to be generated using a far greater number of events than would be feasible with full detector simulation. A fast parameterized detector simulation is developed for this purpose and is described in detail in Ref. [2]. The fast event generation and detector simulation enables reliable estimates of systematic uncertainties since we are able to produce several simulation samples where the relevant parameters are varied within their uncertainty.

The main quantities in the event measured by the detector are the momentum of the charged lepton and the hadronic recoil, the total transverse momentum of the remaining particles, recoiling (in the transverse plane) from the W boson. The measurement of the recoil is necessary to reconstruct the missing transverse momentum $\not\!\!E_T$. Recoiling particles come from gluon radiation of the incoming quarks, and the underlying event processes. The fast event generation and detector simulation have to be calibrated to predict these kinematic variables to a part in 10^4.

2.2. Momentum and Energy Measurement Calibrations

The muon momentum is determined using the Central Outer Tracker (COT), a gas-filled cylindrical drift chamber placed in a 1.4 T magnetic field. The internal alignment of the COT is performed using high-p_T cosmic rays. The fast simulation of the momentum measurement takes into account the energy loss and scattering of particles in the material, COT hit resolutions and the track-fitting algorithm. The absolute momentum measurement scale and hit resolutions as well as the number of simulated radiation lengths of traversed material are tuned on data.

The energy of the electron is obtained from the measurement in the electromagnetic calorimeter (EM), while the angular information of the electron track is obtained with the COT. The simulation of the energy measurement

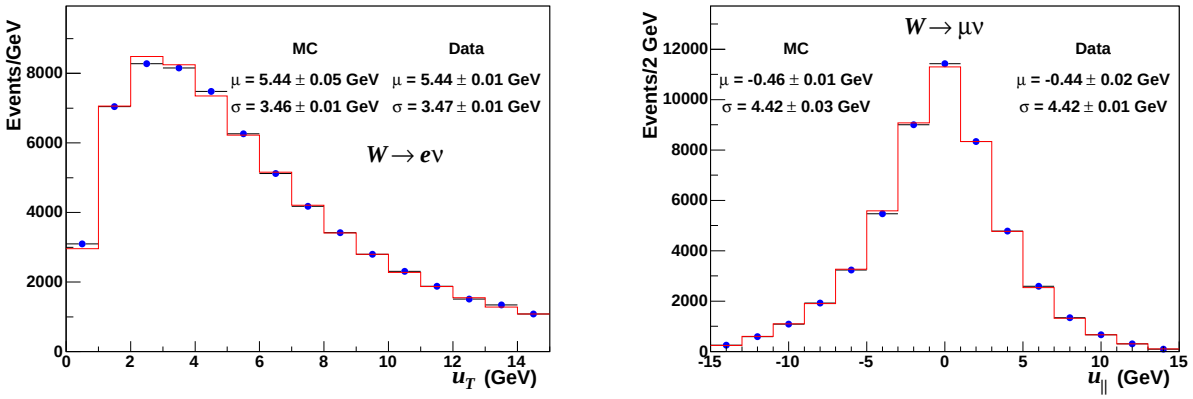

(a) (b)

Figure 2: (a) The comparison of the simulated magnitude of the recoil with data, for $W \to e\nu$ candidates. (b) The comparison of the simulated distribution of the recoil component in the direction of the charged lepton with data, for $W \to \mu\nu$ candidates.

includes the nonlinearity of the calorimeter response, the energy dependence of the energy measurement and the shower leakage out of the EM calorimeter.

The calibration of the measured momenta and energies is one of the most important aspects of the W boson mass measurement, since scaling the measured momenta directly shifts the fitted kinematic distributions. The absolute momentum scale is set by requiring that the measured values of the precisely known masses of the Z, J/ψ and $\Upsilon(1S)$ resonances in the decays to a pair of muons correspond to their PDG values [3]. Figure 1(a) shows that the fractional momentum scale corrections obtained from different invariant mass fits are consistent with each other. Combining the calibration using all three particle masses enables momentum determination with an accuracy of 0.021%.

Taking advantage of the high $J/\psi \to \mu^+\mu^-$ and $\Upsilon(1S) \to \mu^+\mu^-$ statistics, the measured momentum can be calibrated more accurately than the energy measured in the calorimeter. The momentum calibration is hence transferred to the energy measurement using the E/pc distribution (Figure 1(b)). We adjust the absolute energy scale on the peak of the E/pc distribution: the tuning is done in several transverse energy bins to account for non-linear calorimeter response. The number of radiation lengths of material used in the energy loss simulation is tuned to match the radiative tail of the E/pc distribution.

The calibration yields a $Z \to e^+e^-$ mass measurement of $M_Z = 91190 \pm 67_{\rm stat}$ MeV/c^2, in very good agreement with the world average (91187.6 ± 2.1 MeV/c^2 [3]). The calorimeter calibration is further improved by combining the tunes of the E/pc and the $Z \to e^+e^-$ invariant mass distributions. Similar to the scale, the resolution of the energy measurement is tuned on the widths of the E/pc and the $Z \to e^+e^-$ mass distributions.

2.3. Hadronic Recoil Calibration

Simulation of the reconstructed transverse momentum of the neutrino, i.e. the missing transverse momentum $\not\!\!E_T$, requires an accurate simulation of the hadronic recoil, the total transverse momentum of all particles except that of the two prompt leptons from the W boson decay. It is measured from all the energy depositions in the calorimeter, except those associated with the primary charged lepton. These depositions are caused by particles from initial state QCD radiation, the hadronization of the $p\bar{p}$ remnants not partaking in the boson creation, multiple collisions from the same bunch crossing and from initial and final-state photons. The contribution of different components to the magnitude and spread of the recoil distributions is parameterized and the parameterization tuned on the $Z \to \ell^+\ell^-$ decays and minimum bias data (for the underlying event). The comparison of the data and the simulated magnitude of the recoil (Figure 2(a)) and $u_{||}$, the component of the recoil in the lepton direction (Figure 2(b)) shows good agreement. The m_W measurement is specially sensitive to $u_{||}$ as it directly affects the calculation of m_T.

2.4. Generation of W boson production and decay

The dedicated parameterized Monte Carlo simulation has to model both initial state gluon radiation, which is responsible for a non-zero W boson p_T, and the QED radiation of the final state lepton(s). The W boson p_T spectrum is modelled with RESBOS [4] and its parameterization of the non-perturbative low p_T region is tuned on the dilepton p_T distribution in the $Z \to \ell^+\ell^-$ decays. The QED corrections of one-photon emission are simulated using WGRAD [5]. The photon energies are increased by 10% (with an absolute uncertainty of 5%) to account for additional energy loss due to two-photon radiation which is not included in the WGRAD calculation.

Systematic uncertainties due to the limited knowledge of the non-perturbative QCD parameters determining the W p_T spectrum and the simulation of the radiation of more than one photon were estimated (see Table II).

Parton distribution functions (PDFs) are used to calculate the kinematics of the W boson decay products. The CTEQ6M [6] PDFs and their error sets are used for the generation of templates and the PDF uncertainty estimation (Table II).

2.5. Backgrounds

Due to imperfect detector measurement and coverage, several background processes can mimic a $W \to \ell\nu$ decay, thus passing the W event selection. We estimate the amounts and shapes of the dominant background contributions and add them to the simulation templates when performing the m_W fits.

The main backgrounds in the $W \to e\nu$ channel are $Z \to e^+e^-$ and $W \to \tau\nu$ events, and events where a hadronic jet is mis-reconstructed as a lepton ('multi-jet background'). We model $Z \to e^+e^-$ and $W \to \tau\nu$ events using PYTHIA [7] and the full GEANT simulation of the CDF detector. The multi-jet background normalizations are found by fitting the low $\not\!\!E_T$ distribution, where this background dominates.

The main backgrounds in the $W \to \mu\nu$ channel are $Z \to \mu^+\mu^-$ and $W \to \tau\nu$ events, cosmic rays, decays of low momentum pions or kaons into muons in the COT, and hadronic jets, penetrating into the muon chambers or decaying to muons. The $Z \to \mu^+\mu^-$ and $W \to \tau\nu$ events are modelled using PYTHIA and the full detector simulation. The contribution of low momentum meson decays is found by fitting the high tail of the track fit χ^2 distribution where this background is large.

3. W BOSON MASS FITS AND THE RESULT

Finally, the W boson mass is determined separately for the electron and muon channels, in the fits to the three kinematic distributions (m_T, p_T^l and $\not\!\!E_T$). The results of the fits are summarized in Table I. The two transverse mass fits are shown in Figure 3. The breakdown of the systematic uncertainties for the example of the m_T fit is given in Table II.

The six W boson mass fits are combined, taking into account the correlations, to give $m_W = 80413 \pm 34_{\rm stat} \pm 34_{\rm syst}$ MeV/c^2. With a total uncertainty of 48 MeV/c^2, this measurement is the most precise single measurement of m_W to date. This result increases the world average W boson mass to $m_W = 80398 \pm 25$ MeV/c^2 [8], reducing its total uncertainty by 15%.

A global electroweak fit with the new m_W average together with the current best measurement of the top quark mass, $m_t = 172.6 \pm 1.4$ GeV/c^2 [9], constrains the possible Higgs boson mass to $m_H = 86^{+36}_{-27}$ GeV/c^2 [8]. The corresponding 95% confidence level upper limit on the Higgs boson mass is 160 GeV/c^2 [8]. Figure 4 shows the comparison of the m_W and m_t measurements with their constraint on the Higgs boson mass. The m_W and m_t units of the plot reflect how the uncertainty on both masses propagates to the uncertainty on the predicted m_H. To achieve the same level of constraint from W boson and top-quark mass measurements requires their uncertainties to satisfy $\Delta m_W \approx 0.006 \cdot \Delta m_t$. It can be seen from Figure 4 that currently the uncertainty of the m_W measurement is the limiting factor, thus motivating further work.

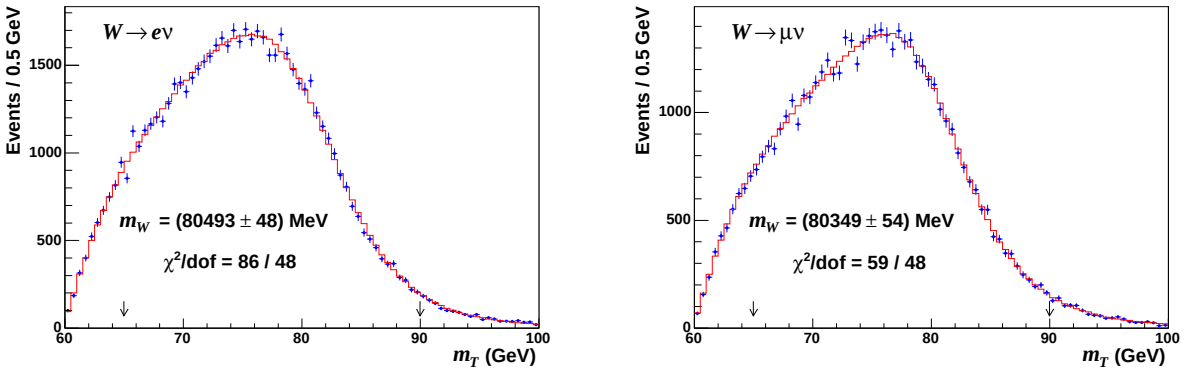

(a) (b)

Figure 3: Transverse mass fit in the $W \to e\nu$ (a) and $W \to \mu\nu$ decay channel (b). The uncertainty given is statistical only. The arrows indicate the limits of the fit range.

The total uncertainty of the published CDF measurement is smaller than it was projected for 200 pb^{-1} from the Run I CDF and DØ measurements, mainly due to the inclusion of the $\Upsilon(1S)$ and J/ψ resonances in the momentum calibration and the usage of the E/pc distribution for the energy measurement calibration. Further improvements in the detector model and the production and decay model (for example QED radiative corrections) are likely to reduce other systematic uncertainties as well. The CDF collaboration therefore predicts that the measurement of the W boson mass with a precision better than that of the current world average (25 MeV/c^2) is possible with the CDF data already in hand.

4. FIRST LOOK AT THE 2.4 fb^{-1} CDF RUN-II DATA

The CDF collaboration has now collected well over ten times more data than were used in the published analysis [2]. Most of the systematic uncertainties in the published measurement (Table II) are limited by the statistics of the calibration samples. The sensitivity of a precision measurement to much higher instantaneous luminosities and the fact that the data from a much longer period of data-taking have to be calibrated, prevent a straight-forward inclusion of more data.

The CDF collaboration has selected a data sample corresponding to approximately 2.4 fb^{-1} that is most suitable

Distribution	m_W (MeV/c^2)	χ^2/dof
$m_T(W \to e\nu)$	$80493 \pm 48_{\rm stat} \pm 39_{\rm syst}$	86/48
$p_T^e(W \to e\nu)$	$80451 \pm 58_{\rm stat} \pm 45_{\rm syst}$	63/62
$p_T^\nu(W \to e\nu)$	$80473 \pm 57_{\rm stat} \pm 54_{\rm syst}$	63/62
$m_T(W \to \mu\nu)$	$80349 \pm 54_{\rm stat} \pm 27_{\rm syst}$	59/48
$p_T^\mu(W \to \mu\nu)$	$80321 \pm 66_{\rm stat} \pm 40_{\rm syst}$	72/62
$p_T^\nu(W \to \mu\nu)$	$80396 \pm 66_{\rm stat} \pm 46_{\rm syst}$	44/62

Table I: Fit results with total systematic and statistical uncertainties from all three fit distributions used to extract m_W.

for the improved m_W measurement and have already performed several calibrations with the data (due to different triggering requirements the $W \to \mu\nu$ and $Z \to \mu^+\mu^-$ decay samples correspond to approximately 2.3 fb^{-1}, as stated on the plots). The following preliminary figures show that the increased luminosity and range of the data samples have neither significantly deteriorated the quality of the collected data nor our ability to measure the quantities of interest.

4.1. Instantaneous Luminosity

Figure 5(a) shows the comparison of the instantaneous luminosity distributions for the published analysis and the preliminary 2.4 fb^{-1} data. Higher average instantaneous luminosities and a much wider distribution of luminosity values affect the modelling of multiple $p\bar{p}$ interactions and backgrounds. The recoil distributions are the ones most severely altered and the recoil simulation now includes the instantaneous luminosity in its parameterization. The dependence of the hadronic recoil on the instantaneous luminosity can be seen in the distributions of ΣE_T, the total recoil energy deposit in the calorimeter. Figure 5(b) shows the comparison of the data and the simulated distribution of ΣE_T for events with instantaneous luminosity smaller and greater than 70×10^{30} s^{-1} cm^{-2} (this value roughly corresponds to the average instantaneous luminosity of the whole sample) for $Z \to e^+e^-$ events. The agreement shows that the parameterizations are able to capture the dependence of the total recoil energy deposition on luminosity.

4.2. Statistical scaling of uncertainties

The degradation of the detector performance and the changes introduced to the detector over time are systematic effects that can spoil the scaling of measurement uncertainties with statistics. Special care has been taken with the data calibrations to keep the quality of the new data comparable to the one in the published analysis.

Syst. uncertainty (MeV/c^2)	$W \to e\nu$	$W \to \mu\nu$	Common
Lepton: Scale	30	17	17
Lepton: Resolution	9	3	0
Recoil: Scale	9	9	9
Recoil: Resolution	7	7	7
Selection	3	1	0
Lepton Removal	8	5	5
Backgrounds	8	9	0
$p_T(W)$ Model	3	3	3
PDFs	11	11	11
QED radiation	11	12	11
Total Systematics	39	27	26
Total Uncertainty	62	60	26

Table II: Systematic and total m_W uncertainties for the transverse mass fits in $W \to e\nu$ and $W \to \mu\nu$ channels. The correlated part of each systematic uncertainty between the two channels is given in the last column. All values in MeV/c^2.

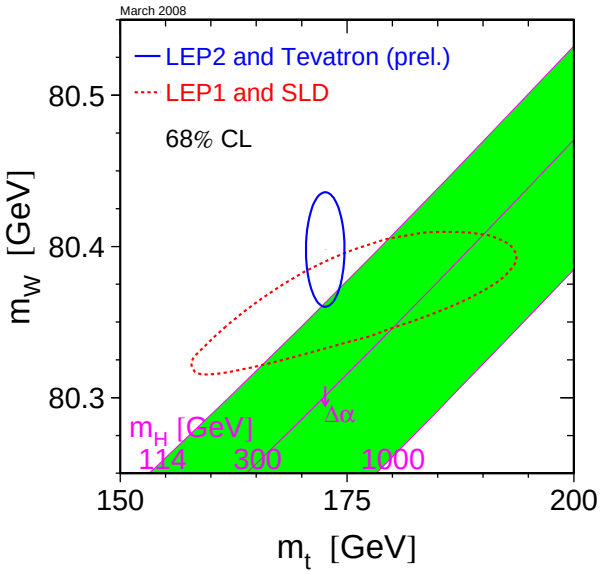

Figure 4: The constraint on the Higgs boson mass from direct m_W and m_t measurements at 68% confidence level (CL). The band shows the SM relationship of the two masses as a function of m_H which can be read from the abscissa.

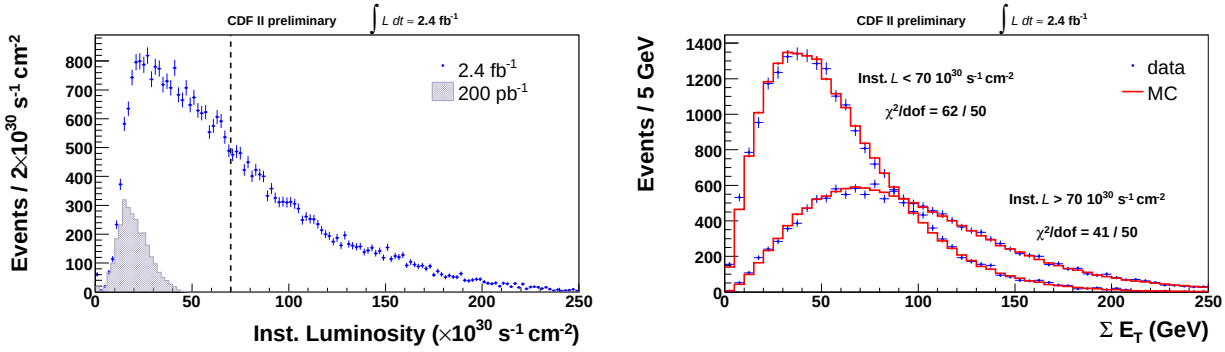

(a) (b)

Figure 5: (a) the comparison o the instantaneous luminosity distributions for the published analysis [2] and the preliminary 2.4 fb^{-1} data. (b) The distribution of ΣE_T for events at instantaneous luminosity greater and smaller than the average instantaneous luminosity of the preliminary 2.4 fb^{-1} dataset. The plots are for $Z \to e^+e^-$ events.

Figures 6 and 7(a) show the invariant mass distributions used for the calibration of the momentum measurement. The fit for the momentum scale in $J/\psi \to \mu^+\mu^-$ decays is done in bins of average curvature, the example plot shown, Figure 6(a) is for the bin corresponding to the muons with the highest reconstructed momenta. Figures 7(b) and 8(b) show the kinematic variables used for the calibration of the energy measurement. The invariant mass of the candidate electrons from the $Z \to e^+e^-$ decays, using only the information from the COT, is shown in Figure 8(a). Due to the significant energy loss suffered by the electrons as they pass through the detector material this distribution has worse Z boson mass resolution than the invariant mass constructed from calorimeter information. Good agreement between data and simulation gives confidence in the simulation of the passage of electrons through the detector. Figure 9 shows the m_T distributions for data and simulation, used in the m_W fit.

The statistical uncertainty of the relevant quantity is obtained from the fits. The statistical uncertainty of the m_W fits of m_T and the m_Z fits of the invariant dilepton mass is obtained from a fit with the simulation blinded

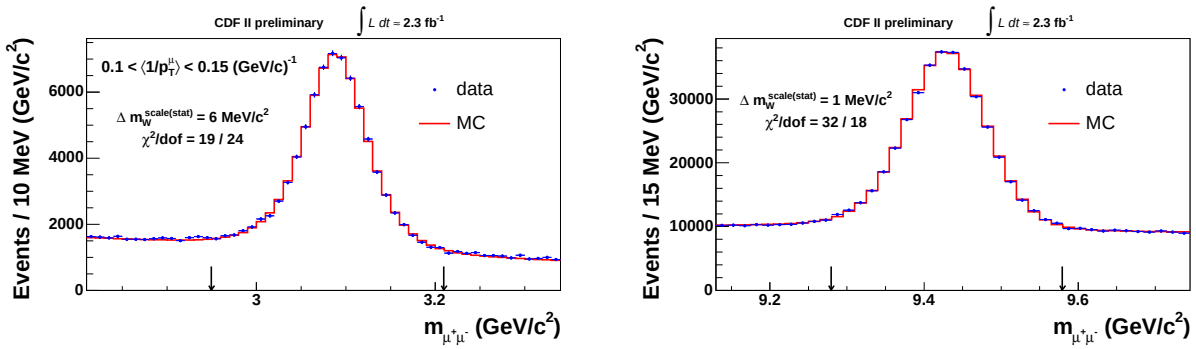

(a) (b)

Figure 6: The invariant dimuon mass for $J/\psi \to \mu^+\mu^-$ (a) and $\Upsilon(1S) \to \mu^+\mu^-$ decays (b). The plot for $J/\psi \to \mu^+\mu^-$ is for muons with highest average momenta. The arrows indicate the limits of the fitting window.

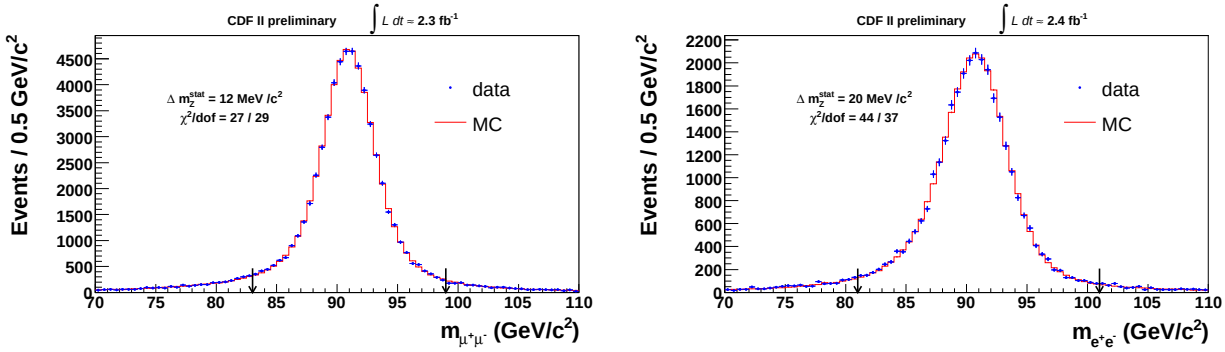

(a) (b)

Figure 7: The invariant dimuon mass for $Z \to \mu^+\mu^-$ (a) and $Z \to e^+e^-$ decays (b). The arrows indicate the limits of the fitting window.

by an unknown additive offset. In Table III the obtained uncertainties are compared to the expected statistical uncertainty obtained by scaling the published result [2] by the square root of the ratio of integrated luminosities. The fit uncertainties show that the resolutions of the distributions in the 2.4 fb^{-1} dataset are comparable to those of the data used in the published result.

5. CONCLUSION

We have published the most precise single measurement of the W boson mass [2]. The total uncertainty of the published CDF measurement is smaller than it was projected from previous measurements, and the improvements in the detector model and the production and decay model will further reduce the systematic uncertainties of future measurements. The CDF has set a goal of measuring the W boson mass with a precision better than that of the current world average (25 MeV/c^2), using a dataset of approximately 2.4 fb^{-1}.

The preliminary plots using 2.4 fb^{-1} show that the expected statistical uncertainty of W mass fits scales with statistics, indicating that the potential degradation of the level of description due to the larger spread of instantaneous luminosities and time-dependent effects has not significantly affected the sensitivity of the fits.

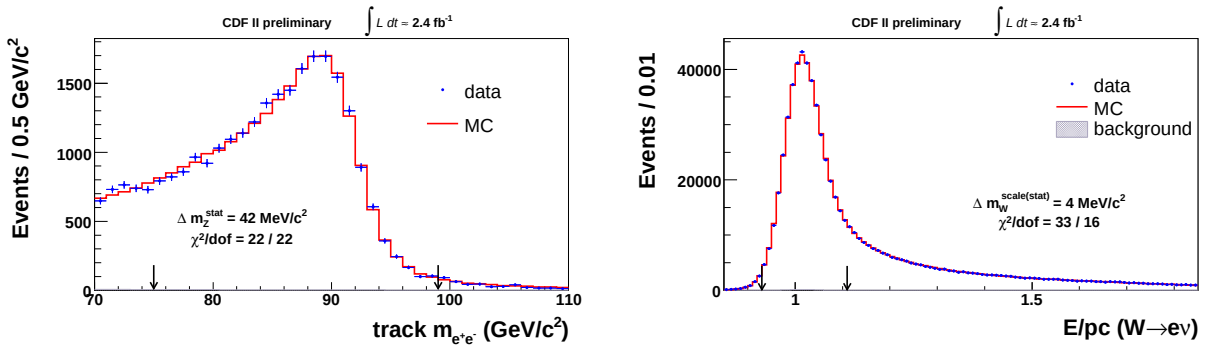

(a) (b)

Figure 8: (a) The invariant mass of the $Z \to e^+e^-$ electron pair, calculated from the momentum information measured in the COT. (b) The E/pc distribution of electrons from $W \to e\nu$ decays. The arrows indicate the limits of the fitting window.

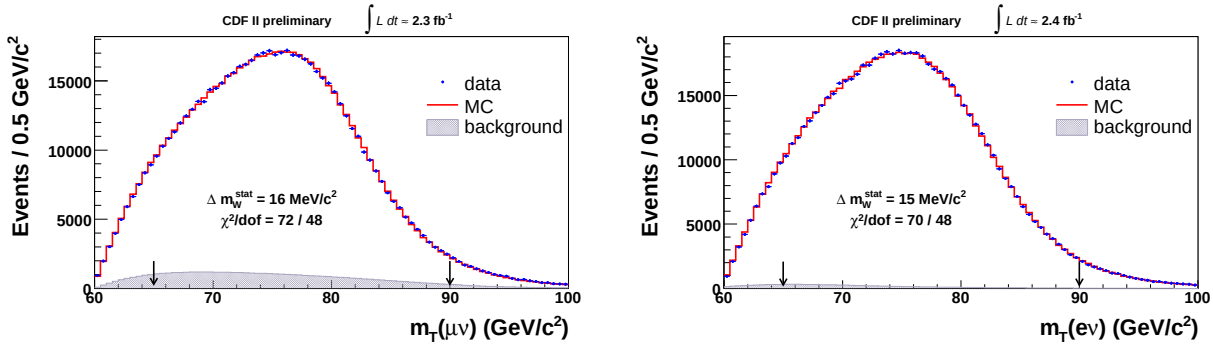

(a) (b)

Figure 9: The transverse mass distribution for $W \to \mu\nu$ (a) and $W \to e\nu$ decays (b). The arrows indicate the limits of the fitting window.

References

[1] V.M. Abazov *et al.* [CDF and DØ Collaborations], "Combination of CDF and DØ results on W boson mass and width," Phys. Rev. D **70**, 092008, (2004).

[2] T. Aaltonen *et al.* [CDF Collaboration], "First Measurement of the W Boson Mass in Run II of the Tevatron," Phys. Rev. Lett. **99**, 151801 (2007) [arXiv:0707.0085v2 [hep-ex]];
T. Aaltonen *et al.* [CDF Collaboration], "First Run II Measurement of the W Boson Mass", Phys. Rev. D **77**, 112001 (2008) [arXiv:0708.3642v1 [hep-ex]].

[3] W. M. Yao *et al.* [Particle Data Group], "Review of particle physics," J. Phys. G **33**, 1 (2006).

[4] C. Balazs and C.-P. Yuan, "Soft gluon effects on lepton pairs at hadron colliders," Phys. Rev. D **56** 5558 (1997).

[5] U. Baur, S. Keller, and D. Wackeroth, "Electroweak radiative corrections to W boson production in hadronic collisions," Phys. Rev. D **59** 013002 (1998).

[6] J. Pumplin, D. R. Stump, J. Huston, H. L. Lai, P. Nadolsky and W. K. Tung, "New generation of parton distributions with uncertainties from global QCD analysis," JHEP **0207** (2002) 012.

[7] T. Sjostrand, S. Mrenna and P. Skands, "PYTHIA 6.4 physics and manual," JHEP **0605**, 026 (2006) [arXiv:hep-ph/0603175].

[8] LEP Collaborations and LEP Electroweak Working Group, http://lepewwg.web.cern.ch/LEPEWWG/.

[9] [CDF and DØ Collaborations], "A Combination of CDF and DØ Results on the Mass of the Top Quark," arXiv:0803.1683 [hep-ex].

uncertainty (all in MeV/c^2)	published 200 pb^{-1}	expected 2.3/2.4 fb^{-1}	prelim. fit 2.3/2.4 fb^{-1}
$\Delta m_Z^{\text{stat.}}(Z \to \mu^+\mu^-)$	43	13	12
$\Delta m_Z^{\text{stat.}}(Z \to e^+e^-)$	67	20	20
$\Delta m_Z^{\text{stat.}}(Z \to e^+e^-{}_{\text{track}})$	143	42	42
$\Delta m_W^{\text{stat.}}(W \to \mu\nu)$	54	16	16
$\Delta m_W^{\text{stat.}}(W \to e\nu)$	48	14	15
$\Delta m_W^{\text{scale(stat.)}}(E/pc,\, W \to e\nu)$	20	6	5
$\Delta m_W^{\text{scale(stat.)}}$(mom. scale, $J/\psi \to \mu^+\mu^-$– one bin)	20	6	6
$\Delta m_W^{\text{scale(stat.)}}$(mom. scale, $\Upsilon(1S) \to \mu^+\mu^-$)	5	1	1

Table III: Statistical scaling, all results in MeV/c^2. The statistical uncertainty for the published result (200 pb^{-1}), the expected statistical uncertainty obtained by scaling the published result by the square root of the ratio of integrated luminosities, and the statistical uncertainty obtained from the presented preliminary fit.